Laboratory photochemical processing of aqueous aerosols: formation and degradation of dicarboxylic acids, oxocarboxylic acids and α-dicarbonyls

C. M. Pavuluri[1], K. Kawamura[1], N. Mihalopoulos[1, 2, 3] and T. Swaminathan[4]

[1]Institute of Low Temperature Science, Hokkaido University, Sapporo 060-0819, Japan

[2]Environmental Chemical Processes Laboratory, Department of Chemistry, University of Crete, P.O. Box 2208, 71003 Voutes, Heraklion, Greece

[3]Institute for Environmental Research and Sustainable Development, National Observatory of Athens, GR-15236 Palea Penteli, Greece

[4]Department of Chemical Engineering, Indian Institute of Technology Madras, Chennai 600036, India

Correspondence to: K. Kawamura (kawamura@lowtem.hokudai.ac.jp)

Abstract. To better understand the photochemical processing of dicarboxylic acids and related polar compounds, we conducted batch UV irradiation experiments on two types of aerosol samples collected from India, which represent anthropogenic (AA) and biogenic aerosols (BA), for time periods of 0.5 h to 120 h. The irradiated samples were analyzed for molecular compositions of diacids, oxoacids and α-dicarbonyls. The results show that photochemical degradation of oxalic (C_2) and malonic (C_3) and other C_8-C_{12} diacids overwhelmed their production in aqueous aerosols whereas succinic acid (C_4) and C_5-C_7 diacids showed a significant increase (ca. 10 times) during the course of irradiation experiments. The photochemical formation of oxoacids and α-dicarbonyls overwhelmed their degradation during the early stages of experiment, except for ω-oxooctanoic acid (ωC_8) that showed a similar pattern to that of C_4. We also found a gradual decrease in the relative abundance of C_2 to total diacids and an increase in the relative abundance of C_4 during prolonged experiment. Based on the changes in concentrations and mass ratios of selected species with the irradiation time, we hypothesize that iron-catalyzed photolysis of C_2 and C_3 diacids dominates their concentrations in Fe-rich atmospheric waters, whereas photochemical formation of C_4 diacid (via ωC_8) is enhanced with photochemical processing of aqueous aerosols in the atmosphere. This study demonstrates that the ambient aerosols contain abundant precursors that produce diacids, oxoacids and α-dicarbonyls, although some species such as oxalic acid decompose extensively during an early stage of photochemical processing.

1 Introduction

Dicarboxylic acids and related polar compounds constitute a significant fraction of water-soluble organic aerosols in the atmosphere (Saxena and Hildemann, 1996; Kawamura and Sakaguchi, 1999; Pavuluri et al., 2010). They have a potential contribution to the formation of cloud condensation nuclei (CCN) due to their water-soluble and hygroscopic properties (Saxena and Hildemann, 1996; Giebl et al., 2002). Thus diacids and related compounds have an impact on the indirect radiative forcing and hydrological cycle (Twomey, 1977; Albrecht, 1989). They also involve in a series of reactions occurring in gas phase, aerosols and atmospheric waters (Chebbi and Carlier, 1996; Wang et al., 2010b). Although diacids, oxoacids and α-dicarbonyls can be directly emitted into the atmosphere from incomplete combustion of fossil fuels (Kawamura and Kaplan, 1987) and biomass burning (Narukawa et al., 1999), they are mainly formed by secondary processes of volatile organic compounds of anthropogenic and biogenic origin (Kawamura et al., 1996a; Kawamura and Sakaguchi, 1999; Kanakidou et al., 2005). They are further subjected to photochemical oxidation during long-range transport; e.g., carbonyls to carboxylic acids (Tilgner and Herrmann, 2010) and breakdown of higher to lower diacids (Kawamura and Sakaguchi, 1999; Matsunaga et al., 1999; Wang et al., 2010a).

Molecular distributions of diacids in atmospheric aerosols have generally been reported with a predominance of oxalic (C_2) acid followed by malonic (C_3) or succinic (C_4) acid in different environments (Kawamura and Kaplan, 1987; Kawamura and Ikushima, 1993; Kawamura and Sakaguchi, 1999; Narukawa et al., 1999; Pavuluri et al., 2010). The predominance of C_2 in different environments is likely explained because it is an ultimate end product in the chain reactions of diacids and various precursors including aromatic hydrocarbons, isoprene, alkenes and α-dicarbonyls (Kawamura et al., 1996a; Warneck, 2003; Ervens et al., 2004b; Lim et al., 2005; Carlton et al., 2007; Charbouillot et al., 2012). In

59 contrast, C_4 was reported to be more abundant than C_2 in some aerosol samples collected
60 from Antarctica (Kawamura et al., 1996b), the Arctic (Kawamura et al., 2010) and over the
61 Arctic Ocean (Kawamura et al., 2012) as well as in ice core samples from Greenland
62 (Kawamura et al., 2001). In addition, a significant reduction in C_2 diacid concentration and an
63 inverse relationship between C_2 and Fe has been reported in stratocumulus clouds over the
64 northeastern Pacific Ocean (Sorooshian et al., 2013). The predominance of C_4 over C_2 in ice
65 core samples and atmospheric aerosols from polar regions, particularly in the Arctic marine
66 aerosol samples collected under overcast conditions with fog or brume event (Kawamura et
67 al., 2012) and the reduction of C_2 in cloud water, suggest that photochemical formation of C_4
68 and/or degradation of C_2 (Pavuluri and Kawamura, 2012) should be enhanced in atmospheric
69 waters.

70 However, the photochemical formation and degradation of diacids and related
71 compounds are not fully understood, particularly in aqueous phase because the composition
72 of aqueous solutions used in laboratory experiments do not reflect the complex mixture of
73 organic and inorganic aerosol constituents in the atmosphere and the experimental conditions
74 are not necessarily atmospherically relevant (Ervens et al., 2011). Hence, it is required to
75 investigate the fate of diacids and related polar compounds with photochemical processing in
76 atmospheric waters. In this study, we conducted a laboratory experiment using two types of
77 ambient aerosol samples collected from Chennai, India, which represent anthropogenic (AA)
78 and biogenic aerosols (BA). The samples were exposed to UV irradiation in the presence of
79 moisture for different time ranging from 0.5 h to 120 h and then analyzed for diacids,
80 oxoacids and α-dicarbonyls. Here, we report their molecular compositions and discuss the
81 photochemical formation and/or degradation of diacids as a function of the irradiation time.
82 Based on the results obtained, we propose possible photochemical formation and degradation
83 pathways of diacids and related compounds with atmospheric implications.

2 Materials and Methods

2.1 Atmospheric aerosol samples

In this study, we used two types of atmospheric aerosol (PM_{10}) samples that were collected in winter on January 28 (IND104) and in summer on May 25 (IND178), 2007 during daytime (ca. 06:00-18:00 h local time) from Chennai (13.03º N; 80.17º E), India using a high volume air sampler and pre-combusted (450 ºC, 4 h) quartz fiber filters. Sampling was conducted on the rooftop of the Mechanical Sciences building (~18 m a.g.l. (above the ground level)) at the Indian Institute of Technology Madras (IITM) campus. The details of sampling site and meteorology are described elsewhere (Pavuluri et al., 2010). The sample filter was placed in a preheated glass jar with a Teflon-lined screw cap and stored in darkness at -20°C prior to the experiment. Figure 1 presents ten-day backward air mass trajectories arriving in Chennai at 500 m AGL for every 6 h during the sampling periods of IND104 and IND178. Table 1 shows concentrations of elemental carbon (EC), organic carbon (OC), levoglucosan and sums of hopanes (specific biomarkers of petroleum and coal) and lipid class compounds: fatty acids and fatty alcohols, in IND104 and IND178 (Fu et al., 2010; Pavuluri et al., 2011).

The air mass trajectories showed that the air masses for the IND104 sample originated from the north Indian subcontinent passing over the Bay of Bengal (Fig. 1). In North India, anthropogenic emissions are mainly derived from fossil fuel combustion and forest fires (Lelieveld et al., 2001; Reddy and Venkataraman, 2002a). This sample is enriched with EC (Table 1). The anthropogenic signature of IND104 is further supported by high abundances of hopanes. In contrast, the air masses for the IND178 sample originated from the Arabian Sea passing over the south Indian subcontinent (Fig. 1), where the emissions from marine biota, combustion of biofuels (e.g., cow-dung) (Reddy and Venkataraman, 2002b) and livestock (Garg et al., 2001) are important. In addition, emission of volatile organic compounds (VOCs)

109 from tropical plant species in India is enhanced in summer (Padhy and Varshney, 2005). This
110 sample is enriched with OC but EC is less abundant (Table 1). The biogenic signature of
111 IND178 is supported by high abundances of fatty acids and fatty alcohols (Table 1). Hence,
112 we consider that IND104 represents anthropogenic aerosols (AA) whereas IND178 represents
113 biogenic aerosols (BA).
114
115 **2.2 Determination of trace elements, metals and water-soluble iron species**
116 Trace elements and metals were determined using an inductively coupled plasma mass
117 spectrometry (ICP-MS, Thermo Electron X Series) after the acid microwave digestion of
118 samples (a filter disc of 1.8 cm in diameter) as reported by Theodosi et al. (2010b).
119 Recoveries obtained with the use of certified reference materials ranged from 90.0 to 104.1%.
120 Water-soluble iron (Fe_{WS}: sum of Fe^{2+} and Fe^{3+} species) was determined spectrometrically
121 using the Ferrozine colorimetric method developed by Stookey (1970) as reported by
122 Theodosi et al. (2010a). Fe^{2+} was measured using the same procedure without adding the
123 reducing agent (hydroxylamine hydrochloride), and then Fe^{3+} was estimated indirectly as the
124 difference between Fe_{WS} and Fe^{2+}. The recovery was ~98.3% for both Fe_{WS} and Fe^{2+}.
125
126 **2.3 Irradiation experiment of aerosol samples**
127 Batch UV irradiation experiments using two aerosol samples (AA and BA) were conducted
128 separately for 0.5, 1.5, 3.0, 6.0, 12, 18, 24, 36, 48, 72, 96 and 120 h, because both primary
129 and secondary chemical species that are associated with aerosols can be subjected for
130 significant photochemical processing through out their stay (i.e., up to 12 days) in the
131 atmosphere (Warneck, 2003). In each experiment, ~12 cm^2 (ca. 3 × 4 cm) of sample filter
132 was cut into 3~4 pieces and placed vertically in a cleaned quartz reaction vessel (cylinder,
133 100 ml) with the sample surface facing to UV light as depicted in Fig. 2. The sample was

fully wetted by injecting ~0.4 ml of ultra pure organic free Milli Q water and sealed with Teflon-lined screw cap under the ambient pressure. Further, the available excess Milli Q water (Fig. 2) may promote humid (RH = 100%) environment in the reaction vessel by equilibrium between water vapor and Milli Q water. The aqueous ambient aerosol sample was then irradiated with a low-pressure mercury lamp (Ushio, UL0-6DQ) that emits a UV, whose spectra are characterized by main peak at 254 nm and minor peak at 185 nm as well as broad peak at >254 nm. The experimental setup (Fig. 2) was covered with a cartoon box containing a hole on each side for the passage of ambient air, and placed in a draft chamber. The temperature around the experimental system (i.e. inside cartoon box) was equivalent to room temperature (25±1°C).

The main objective of UV irradiation with a wavelength primarily at 254 nm, rather than a solar spectrum, was to produce significant amount of hydroxyl radicals ($HO^{\bullet}$) from various sources described below that should be sufficient enough to act as the main oxidant in our experimental system. Although we do not preclude a minor photolysis of some organic compounds present in the aerosol samples by irradiation at ≤254 nm, it is well established that low molecular weight diacids, oxoacids and α-dicarbonyls including pyruvic acid and methylglyoxal have negligible absorbance at 254 nm and exhibit minimal photolysis, particularly when $HO^{\bullet}$ reactions of organics are significant (Carlton et al., 2006; Yang et al., 2008b; Tan et al., 2012). Because sulfate is abundant in non-irradiated AA and BA (Pavuluri et al., 2011), the production of organosulfates should be significant upon irradiation (Noziere et al., 2010) in both the samples. However, the sulfate contents may not have significant impact on the production rate of diacids and related compounds (Tan et al., 2009).

Further, the photolysis of organics by the radiation of 185 nm, whose intensity is 100 times lower than that of 254 nm, should be insignificant during the experiment because the 185 nm light intensity is small and is mostly absorbed by water due to its high absorption

159 coefficient (1.8 cm^{-1} at 25 °C) (Weeks et al., 1963). It is well established that the photolysis
160 rates of organics by the radiation of 185 nm are elevated only in the absence of dissolved
161 oxygen (Shirayama et al., 2001) whereas in aerated solutions, mainly water undergoes
162 photolysis under irradiation of 185 nm and produce the hydrogen atoms, which are scavenged
163 by oxygen to form $HO_2^{\bullet}$ radicals that finally converted to $HO^{\bullet}$ (Chitose et al., 2003; Yang et
164 al., 2008b). Thus, the minor 185 nm light emitted from UV source promotes the production
165 of $HO^{\bullet}$ during the experiment rather than the photolysis of the compounds of interest in this
166 study. On the contrary, iron-dicarboxylate complexes (e.g., oxalate and malonate) can
167 photolyze by absorbing both UV-C (254 nm) and UV-A light and their photolysis rate
168 depends on the concentration of Fe in the given sample rather than the UV light wavelength
169 (Zuo and Hoigne, 1994; Wang et al., 2010b; Pavuluri and Kawamura, 2012). In addition,
170 radiation at 254 nm has been reported to impose only a marginal photolysis of most of the
171 inorganic species, except for nitrate, which is one of the $HO^{\bullet}$ sources (Yang et al., 2008b).
172 The irradiation of wetted aerosol sample at 254 nm induces the formation of O_3 from
173 the dissolved O_2 followed by generation of H_2O_2, and photolysis of H_2O, NO_3^-, NO_2^-, H_2O_2,
174 $Fe(OH)^{2+}$ and certain organic compounds, and Fenton's reaction of photochemically formed
175 Fe^{2+} and H_2O_2 to produce $HO^{\bullet}$ in aqueous phase (Arakaki and Faust, 1998; Carlton et al.,
176 2006; Yang et al., 2008b). In fact, high amount of Fe, including water-soluble Fe^{2+} and Fe^{3+}
177 species, is available in both AA and BA samples (Table 1), which could promote the
178 Fenton's reaction upon UV irradiation. In addition, O_3, H_2O_2, $HOO^{\bullet}$ and NO_2 formed in
179 aqueous phase reactions may be partitioned into gas phase and generate the gaseous $HO^{\bullet}$ that
180 should be re-partitioned into aqueous phase (Arakaki and Faust, 1998). These sources of $HO^{\bullet}$
181 are similar to those of atmospheric waters: (i) gas/drop partitioning of $HO^{\bullet}$ and (ii) gas/drop
182 partitioning of O_3 followed by reaction with peroxy radical ($HOO^{\bullet}$), (iii) photolysis of H_2O,

183 NO_3^-, NO_2^-, H_2O_2, $Fe(OH)^{2+}$ and certain organic compounds, and (iv) Fenton's reaction of
184 Fe^{2+} and H_2O_2 (Arakaki and Faust, 1998).

185 Unfortunately, we could not approximate the actual concentrations of $HO^{\bullet}$ in our
186 experiments because we did not add any chemical (e.g., a standard compound whose kinetics
187 are known) in order to keep our experimental system as realistic as possible. Furthermore, the
188 formation of O_3 from the initially available O_2 (~0.94 mM) in the reaction vessel may not
189 cause the deficit of the O_2 that could potentially induce the polymerization of organics during
190 the irradiation on aerosols for several hours, because the additional O_2 could be produced
191 from the gaseous $HOO^{\bullet}$ formed by photolysis of organics and Fenton's reaction (Arakaki and
192 Faust, 1998) during the experiment.

193

194 **2.4 Measurements of diacids, oxoacids and α-dicarbonyls**

195 Immediately after the irradiation, samples were analyzed for diacids, oxoacids and
196 α-dicarbonyls using a method reported elsewhere (Kawamura, 1993; Kawamura and
197 Ikushima, 1993). Briefly, the irradiated sample filter was extracted with Milli-Q water (10
198 mL x 3) under ultra sonication for 10 min and the extracts were concentrated to near dryness
199 using a rotary evaporator under vacuum. The extracts were then derivatized with 14%
200 BF_3/n-butanol at 100°C to butyl esters and/or butoxy acetals. Both the esters and acetals were
201 extracted with *n*-hexane and then determined using a capillary GC (HP 6890) and GC-MS
202 (Thermo Trace MS). Recoveries of authentic standards spiked to a pre-combusted quartz
203 fiber filter were 73% for oxalic (C_2) acid and more than 84% for malonic (C_3), succinic (C_4)
204 and adipic (C_6) acids (Pavuluri et al., 2010). The analytical errors in duplicate analysis of the
205 aerosol filter sample are within 9% for major species. Gas chromatogram of the field and
206 laboratory blanks showed small peaks for C_2, phthalic (Ph) and glyoxylic acids.

Concentrations of all the species reported here are corrected for the non-irradiated field blanks (Pavuluri et al., 2010).

2.5 Quality control

To examine the possible experimental errors, including the distribution of organic/inorganic constituents over the filter sample, we conducted replicate experiments (n = 3) for 18 h irradiation of AA sample by using the sample cut taken from different parts of the filter sample for each experiment because a deviation in the results of the irradiation experiment should become large if the impact of potential variance in chemical composition of aerosol at different parts of the single filter, size of the filter sample used (i.e., amount of aerosols) and the amount of Milli Q water added is significant. The experimental errors, including the analytical errors, were found to be within 11% for major species, except for C_3 diacid (19%). These results suggest that organic and inorganic constituents are well distributed over the filter sample and took up water evenly distributed upon wetting. In addition, two irradiation experiments were conducted to check the procedural blank by using a clean quartz filter for 1.5 h and 6.0 h. No peaks were detected, except for a small peak for C_2 and Ph. These results indicate that the occurrence of bias during the experiment is insignificant.

3 Results and discussion

3.1 Concentrations of trace elements, metals and water-soluble iron species

Concentrations of trace elements, metals and water-soluble Fe species (Fe^{2+} and Fe^{3+}) determined in non-irradiated AA and BA samples are presented in Table 1. The trace elements and metals in AA sample, which mainly originate from soil dust (e.g., P, Al, Ca and Fe), non-ferrous metallurgical industrial activities (Cd, Cu and Zn) and fossil fuel combustion (Cr, Pb and V) (Pacyna and Pacyna, 2001; Mahowald et al., 2008), are significantly more

232 abundant than in BA (by up to several times higher), except for S, Ni and Sb (Table 1). The
233 high abundances of trace metals in AA further suggest that the AA sample should contain
234 high abundances of anthropogenic organic matter. The high abundances of S, Ni and Sb in
235 BA than in AA may be due to high emissions of the S from intensive consumption of biofuels,
236 particularly cow-dung that contains higher S content (Reddy and Venkataraman, 2002b),
237 while Ni and Sb are from some specific industrial activities in southern India. Although
238 water-soluble Fe^{2+} and Fe^{3+} species are abundant in both AA and BA, their concentrations in
239 BA are 30-50% higher than in AA (Table 1). Further the fraction of water-soluble Fe (Fe_{WS}:
240 sum of Fe^{2+} and Fe^{3+}) in total particulate Fe (Fe_{Tot}) is 2.77% in AA whereas it is 14.6% in
241 BA.
242
243 **3.2 Molecular compositions of diacids, oxoacids and α-dicarbonyls**
244 A homologous series of normal (C_2-C_{12}) and branched chain (iso C_4-C_6) saturated
245 α,ω-diacids were detected in both non-irradiated and irradiated AA and BA samples as well
246 as aliphatic unsaturated diacids such as maleic (M), fumaric (F), and methylmaleic (mM)
247 acids and aromatic diacids such as phthalic (Ph), isophthalic (*i*-Ph), and terephthalic (*t*-Ph)
248 acids. Diacids with an additional functional group, i.e., malic (hydroxysuccinic, hC_4),
249 ketomalonic (kC_3), and 4-ketopimelic (kC_7) acids, were detected, together with ω-oxoacids
250 (ωC_2-ωC_9), pyruvic acid (Pyr), and α-dicarbonyls, i.e., glyoxal (Gly) and methylglyoxal
251 (MeGly). ωC_6 will not be reported here due to the overlapping peak on GC chromatogram.
252 Oxalic (C_2) acid was found as the most abundant diacid in non-irradiated samples
253 (accounting for 54% of total diacids in AA and 53% in BA), followed by Ph (10%), C_4 (9%),
254 C_3 (8%) and C_9 (4%) in AA and by malonic (C_3) (9%), C_4 (6%) and *t*-Ph (6%) acids in BA.
255 Branched chain diacids were significantly lower than the corresponding normal structures in
256 both samples. Glyoxylic (ωC_2) acid is the most abundant oxoacid, comprising 64% and 57%

257 of total oxoacids in AA and BA, respectively, followed by Pyr (13%) and 4-oxobutanoic
258 (ωC_4) acid (10%) in AA and ωC_4 (18%) and Pyr (13%) in BA. MeGly is more abundant than
259 Gly in AA whereas their abundances are equivalent in BA.
260
261 **3.3 Changes in concentrations of diacids and related compounds as a function of UV**
262 **irradiation time**
263 Changes in concentrations of individual and total diacids as a function of UV irradiation time
264 in AA and BA are depicted in Fig. 3, while those of oxoacids and α-dicarbonyls as well as
265 total oxoacids and α-dicarbonyls in Fig. 4. Concentrations of C_2 diacid were sharply
266 decreased by a factor of 3-9 (from 553 ng m^{-3} to 61.7 ng m^{-3} in AA and from 339 to 118 ng
267 m^{-3} in BA) within 6 h and 12 h of UV irradiation, respectively (Fig. 3a). Then, the
268 concentrations started to increase to maximize at 24 h (292 ng m^{-3}) in AA and 18 h (306 ng
269 m^{-3}) in BA on further irradiation. They gradually decreased toward the end (120 h) of the
270 experiment (Fig. 3a). Interestingly, C_3 diacid showed a temporal variation similar to C_2 in
271 both AA and BA, except for few points (Fig. 3b). Relative abundances of C_2 in total diacids
272 gradually decreased from non-irradiated samples (54% in AA and 53% in BA) toward the
273 end (120 h) of the experiment (3.2% in AA and 9.2% in BA, Fig. 5).
274 Concentrations of ωC_2, an immediate precursor of C_2 (Kawamura et al., 1996a;
275 Warneck, 2003; Lim et al., 2005), increased with irradiation time up to 18 h in both AA and
276 BA, except for two cases (3 and 6 h) of AA, and then gradually decreased until the end (120
277 h) of the experiment, except for one case (36 h) in AA (Fig. 4a). Pyr, Gly and MeGly, which
278 are the precursors of ωC_2 acid, are all produced by the oxidation of VOCs of anthropogenic
279 and biogenic origin (Warneck, 2003; Ervens et al., 2004b; Lim et al., 2005; Carlton et al.,
280 2006). They also increased with irradiation time up to 18~24 h in both samples and then
281 gradually decreased (except for MeGly in AA) until the end (120 h) of the experiment (Fig.

4g, i, j). However, the other precursor of C_2 diacid, kC_3 diacid (Kawamura et al., 1996a), showed a decrease with irradiation time throughout the experiment, except for few cases (Fig. 3v) whereas hC_4, a precursor of C_3 diacid (Kawamura et al., 1996a), increased up to 18 h in BA and 24 h in AA and remained relatively high until 72 h and then gradually decreased until the end (120 h) of the experiment (Fig. 3u).

In contrast, concentrations of C_4 diacid showed a gradual increase with irradiation time up to 72 h in BA and 96 h in AA followed by a slight decrease in the AA and a sharp decrease in BA (Fig. 3c). Relative abundance of C_4 diacid in total diacids also increased from 8.9% (non-irradiated) to 82% (120 h) in AA and from 6.4% to 88% in BA (Fig. 5). Similarly, C_5 diacid in AA (Fig. 3d) showed a gradual increase with irradiation up to 36 h and stayed almost constant until 96 h followed by a slight decrease. Similar trend was found in BA (Fig. 3d). Both C_6 and C_7 diacids showed an increase with irradiation up to 6~36 h and then a gradual decrease until the end (120 h) of the experiment (Fig. 3e,f). Concentrations of iC_4 diacid also increased with irradiation up to 18 h in BA and 36 h in AA and stayed relatively constant until 72 h or 96 h. Then, the concentrations gradually decreased until the end (120 h) of the experiment (Fig. 3l). iC_5 and iC_6 diacids (Fig. 3m,n) showed very similar trend with their corresponding normal diacids (Fig. 3d,e).

Long-chain (C_8-C_{12}) diacids showed a sharp decrease with irradiation up to 12 h and then a gradual decrease until the end (120 h) of the experiment (Fig. 3g-k). C_8, C_9 and C_{12} diacids became below the detection limit within several hours, particularly in BA. On the other hand, unsaturated aliphatic (M, F, mM, and Ph) and aromatic diacids (*i*-Ph and *t*-Ph) showed a gradual decrease with irradiation, except for few cases during the early stages of the experiment (Fig. 3o-t). Concentrations of kC_7 increased with irradiation time up to 18 h and then decreased gradually until 120 h (Fig. 3w) whereas oxoacids: ωC_3, ωC_7 and ωC_9 acids, showed a gradual decrease with irradiation, except for few cases (Fig. 4b,d,f). On the other

hand, ωC_4 acid showed a sharp increase up to 12 h and then a sharp decrease toward 24 h (Fig. 4c). Interestingly, temporal pattern of ωC_8 acid (Fig. 4e) was similar to that of C_4 diacid (Fig. 3c).

Thus the changes in the concentrations of individual diacids, oxoacids and α-dicarbonyls as well as relative abundances of individual diacids in total diacids and mass ratios of selected species in AA and BA found to be similar (Figs. 3-6), although significant differences are recognized between AA and BA samples during irradiation. Such similarities in the temporal variations of diacids and related polar compounds infer that their photochemical formation and degradation pathways in aqueous aerosols (Fig. 7) are almost same between anthropogenic and biogenic aerosols. However, there were significant differences in the rate of formation and/or degradation of diacids and related compounds between AA and BA, which might have been driven by the differences in the abundances of the diacids and related compounds as well as their precursor compounds in the original (non-irradiated) AA and BA samples. In fact, total diacids, oxoacids and α-dicarbonyls were higher in non-irradiated AA than in BA. On the contrary, OC that contains several precursor compounds (including fatty acids) of diacids and related polar compounds is higher in BA than in AA (Table 1).

3.4 Production and decomposition of short-chain diacids and related compounds

A sharp increase was observed in the concentrations of ωC_2, ωC_4, Pyr, Gly and MeGly, but not ωC_3, with irradiation up to 18~24 h following a gradual decrease (Fig. 4), demonstrating an enhanced photochemical production of short-chain ($\leq C_4$) oxoacids and α-dicarbonyls during an early stage of photochemical processing. It is likely because ωC_2, Pyr, Gly and MeGly are significantly produced by photochemical oxidation of aliphatic olefins and aromatic hydrocarbons whereas ωC_4 from cyclic olefins and unsaturated fatty acids (Bandow

et al., 1985; Hatakeyama et al., 1987; Kawamura et al., 1996a; Warneck, 2003; Lim et al., 2005) but ωC_3 may not be significantly produced from any of these precursor compounds (Fig. 7). On the other hand, the increasing trends of mass ratios of C_2 to its precursor compounds: ωC_2, Pyr, Gly and MeGly as well as C_3 (but not C_4) diacid (Kawamura et al., 1996a; Warneck, 2003; Ervens et al., 2004b; Lim et al., 2005; Carlton et al., 2007), were found for BA toward to 120 h (Fig. 6a-e and f). It is noteworthy that $C_3/\omega C_7$ ratios also showed a slight increase, although they are not clear in the later stages of experiment (Fig. 6g), suggesting a potential formation of C_3 diacid via ωC_7 that is derived from unsaturated fatty acids and/or cyclic olefins. In addition, F/M ratios showed an increase with irradiation up to 48 h in AA and 18 h in BA followed by a gradual decrease until the end of experiment (Fig. 6i), indicating a significant photochemical transformation during an early stage of experiment and decomposition in a later stage.

Photochemical degradation of C_2 and C_3 diacids should have overwhelmed their photochemical production even in an early stage of experiment, except for few cases (Fig. 3a,b). Diacids and other compounds containing a carbonyl group can form stable carboxylate salts with amines upon photochemical oxidation. However, based on laboratory studies, C_2 and C_3 diacids have been reported to decompose in aqueous phase in the presence of Fe^{3+} (and C_2 diacid even in the presence of Fe^{2+}) under UV irradiation at 254 nm as well as at a solar spectrum (>300 nm) (Zuo and Hoigne, 1994; Wang et al., 2010b; Pavuluri and Kawamura, 2012), but C_2 diacid (and maybe C_3 diacid) is relatively stable in the absence of Fe species (Pavuluri and Kawamura, 2012). It is well documented that both C_2 and C_3 diacids have the strongest chelating capacity with Fe^{3+} among all diacids and tend to form mono, di and tri oxalato (equilibrium constant $\log_{10}(b) = 9.4$, 16.2 and 20.4, respectively) and malonato (equilibrium constant $\log_{10}(b) = 7.5$, 13.3 and 16.9, respectively) complexes by acting as ligands in aqueous phase, which exhibit a strong light absorbing ability (Wang et al., 2010b).

Although the equilibrium constant of Fe^{3+}-malanato complex is slightly lower than that of Fe^{3+}-oxalato, both diacids photolyze upon the absorption of UV light to result in Fe^{2+} and CO_2 (Zuo and Hoigne, 1994; Wang et al., 2010b).

We found that non-irradiated AA and BA samples contain significant amounts of water-soluble Fe^{2+} and Fe^{3+} species (Table 1). Because high abundance of particulate Fe is present in both AA and BA (Table 1), the concentrations of water-soluble Fe^{2+} and Fe^{3+} species in both AA and BA samples may increase upon UV irradiation; the water-insoluble Fe can be transformed into water-soluble forms by photochemical processing of mineral aerosols (Solmon et al., 2009; Srinivas et al., 2012). However, we did not measure the concentrations of Fe^{2+} and Fe^{3+} species in the irradiated samples. In fact, the mass ratio of C_2 diacid to Fe^{3+} is 15:1 in non-irradiated AA and 7:1 in BA, which are close to the ratio (10:1) used in laboratory experiments conducted by Pavuluri and Kawamura (2012) for Fe-catalyzed photolysis of C_2 diacid in aqueous phase, in which the photolysis of C_2 is very fast ($k = 206$ L mol^{-1} s^{-1}) and 99% of the C_2 is degraded in 0.5 h. Therefore, available water-soluble Fe^{3+} (and Fe^{2+}) in AA and BA should be enough to promote the catalytic photochemical degradation of C_2 (and C_3) upon UV irradiation (Fig. 7) and thus the degradation rate of C_2 (and C_3) should have increased with the prolonged experiment due to enhancement in Fe^{3+} (and Fe^{2+}) levels in the given sample.

The concentration of C_2 diacid in AA decreased by 30% in 1.5 h and continued to decline by 90% until 12 h (Fig. 3a). On the other hand, the experiment of BA showed that the concentration of C_2 decreased by 47% and 51% in 0.5 h and 1.5 h, respectively, and then gradually declined. The concentrations of C_3 also showed similar trends with C_2 (Fig. 3b). Although C_2 and C_3 diacids decreased sharply during early stages of experiment, they decreased gradually in the later stages, despite possibly enhanced levels of water-soluble Fe^{2+} and Fe^{3+} species. These trends imply that photolysis of C_2 and C_3 diacids is highly significant

382 in the presence of water-soluble Fe^{3+} (and Fe^{2+}) (Fig. 7). On the other hand, the formation of
383 both C_2 and C_3 diacids is also intensive with the photochemical processing of their precursor
384 compounds in AA and BA. However, the net rate of production or degradation of C_2 and C_3
385 diacids in each experiment (Figs. 3a,b) should depend on the abundances of water-soluble
386 Fe^{2+} and Fe^{3+} species and their precursors in AA and BA.

387 We found an increase in the mass ratios of MeGly to Gly with irradiation toward the
388 end of the experiment, except for an early stage of experiment (up to 6 h) in AA, whereas in
389 BA they remained relatively constant up to 36 h and then increased gradually up to 72 h
390 followed by a rapid decrease (Fig. 6n). As noted earlier, concentrations of Gly and MeGly
391 increased with experiment up to 18~24 h in both AA and BA. Thereafter, Gly decreased
392 toward the end of experiment in both AA and BA whereas MeGly remained relatively
393 constant in the AA, but decreased in BA (Fig. 4i,j). Such differences should be caused by the
394 difference in their production rates depending on the concentrations of potential precursors
395 and their oxidation products in AA and BA: benzene and glycolaldehyde for Gly, acetone and
396 higher alkanes ($>C_3$) and alkenes ($>C_2$) for MeGly (Fu et al., 2008), rather than the reaction
397 rates of the Gly (1.1×10^9 M^{-1} S^{-1}) and MeGly (6.44×10^8 M^{-1} S^{-1}) with $HO^{\bullet}$ in aqueous
398 phase (Tan et al., 2012). Therefore, the high abundance of MeGly in AA than Gly can be
399 attributed to its enhanced production than the later species during photochemical processing
400 of aqueous aerosols derived from anthropogenic sources. Further, the oligomerization of Gly
401 and MeGly (Tan et al., 2009; Lim et al., 2010; Tan et al., 2012) might have also played an
402 important role on the changes in their concentrations with irradiation time, however, we did
403 not focus on the measurements of oligomers here because of the analytical limitations.
404

405 **3.5 Possible photochemical pathways of long-chain diacids and oxoacids**

406 Enhanced concentrations of normal and branched C_4-C_7 diacids during an early stage
407 (18~36 h) (Fig. 3c-f), despite degradation of C_2 and C_3 and longer-chain >C_7) diacids (Fig. 3a,
408 b, g-k), may be caused by photochemical oxidation of the first generation products derived
409 from the oxidation of anthropogenic and/or biogenic VOCs (e.g., cycloalkenes, monoterpenes,
410 and sesquiterpenes) and unsaturated fatty acids (Kalberer et al., 2000; Gao et al., 2004) (Fig.
411 7). In addition, the photochemical oxidation of the polymers of polyunsaturated fatty acids, if
412 available, can significantly produce the long-chain ($\geq C_4$) diacids (Harvey et al., 1983), a
413 subject of future research. In fact, polyunsaturated fatty acids (e.g., linolenic acid ($C_{18:3}$)) can
414 undergo free radical oxidative cross-linking in the air and produce high molecular weight
415 organic compounds (e.g., fulvic acid) (Wheeler, 1972; Harvey et al., 1983). Harvey et al.
416 (1983) found a series of C_4-C_9 diacids by oxidizing the marine fulvic acid in a laboratory
417 study. On the other hand, the chelating capability of succinate (equilibrium constant $\log_{10}(b)$
418 = 7.5 (Wang et al., 2010b)) and other long-chain diacids with Fe^{3+} is weak and hence, their
419 photolysis is insignificant. However, they should be further oxidized to result in lower diacids
420 (Kawamura et al., 1996a; Matsunaga et al., 1999). The degradation of these diacids should be
421 increased with increasing chain length because the oxidation rate of C_4 to C_9 diacids is
422 increased with increasing carbon number (Yang et al., 2008a).
423 The relatively constant levels of C_5, *i*C_4 and *i*C_5 during 36 h and 72~96 h (Fig. 3d, l,
424 and m) may be due to the balance between photochemical production and degradation. The
425 increases in the concentrations of C_4 with a prolonged irradiation up to 72 h in BA and 96 h
426 in AA further demonstrate its formation from higher diacids and other precursors in aqueous
427 aerosols (Kawamura and Sakaguchi, 1999; Charbouillot et al., 2012) (Fig. 7). In fact, total
428 diacids stayed relatively constant from 24 h to 72~96 h (Fig. 3x). In addition, mass ratios of
429 C_4 to C_5-C_7 showed a gradual increase throughout the experiment (until 120 h) in both AA
430 and BA (Fig. 6k-m). These results support a photochemical breakdown of longer-chain ($\geq C_5$)

diacids resulting in C_4 (Matsunaga et al., 1999; Yang et al., 2008a; Charbouillot et al., 2012). Yang et al. (2008a) reported that the production of C_4 diacid is predominant followed by C_5 diacid during a laboratory photochemical oxidation of C_6-C_9 diacids.

In addition, ωC_8 acid, which can be produced by the oxidation of cyclic olefins and unsaturated fatty acids (Kawamura and Sakaguchi, 1999; Gao et al., 2004), showed a gradual increase (Fig. 4e) similar to that of C_4 diacid (Fig. 3c) in both AA and BA, suggesting a significant photochemical production of C_4 via ωC_8 until the consumption of the precursor compounds derived from anthropogenic and biogenic VOCs and biogenic unsaturated fatty acids (Kalberer et al., 2000; Gao et al., 2004). In fact, ratios of C_4 to C_5-C_7 were 10 times higher in BA than in AA whereas those of $C_4/\omega C_8$ were similar in both the BA and AA (Fig. 6j). However, their temporal profiles with irradiation time are similar in both AA and BA. These results suggest that the formation of C_4 and ωC_8 is much higher in biogenic aerosols than in anthropogenic aerosols compared to C_5-C_7 diacids, but their formation/degradation processes may be similar irrespective of the origin of precursors. However, it is not clear from this study if C_4 is mainly derived (via ωC_8) from cyclic olefins or unsaturated fatty acids (Fig. 7).

It is well established that long-chain (C_8-C_{12}) diacids are formed by photochemical oxidation of unsaturated fatty acids (e.g., oleic acid) (Kawamura and Gagosian, 1987; Matsunaga et al., 1999) (Fig. 7). However, unsaturated fatty acids were not abundant (e.g., oleic acid was 0.89 ng m^{-3} in AA and below detection limit in BA) in non-irradiated samples (Fu et al., 2010). Hence, photochemical formation of long-chain diacids from the oxidation of unsaturated fatty acids should be less important during the experiment, although chemical forms of polymerized and/or partially oxidized unsaturated fatty acids may be abundant in the aerosols. On the other hand, photooxidation rate constant of diacids increases with an increase in carbon number of individual diacids ($\geq C_4$) (Yang et al., 2008a). Hence,

456 photochemical breakdown of C_8-C_{12} diacids to lower diacids (Matsunaga et al., 1999; Yang
457 et al., 2008a) should be very likely (Fig. 7). The gradual decreases of aliphatic unsaturated
458 diacids, aromatic diacids, and oxoacids, except for ωC_8, with irradiation are likely caused by
459 the photochemical degradation (Fig. 7).
460
461 **3.6 Atmospheric implications**
462 As discussed above, this study reveals that photochemical degradation of C_2 and C_3 (due to
463 Fe-catalyzed photolysis) in aqueous aerosols overwhelmed their production whereas C_4
464 diacid showed photochemical formation. These results are consistent with the recent
465 atmospheric observations: a significant reduction in C_2 diacid concentration and an inverse
466 relationship between the C_2 and Fe in cloud water (Sorooshian et al., 2013), and the
467 replacement of the predominance of C_2 by C_4 in the Arctic aerosols (Kawamura et al., 2010;
468 Kawamura et al., 2012). It was also reported that C_4 and C_5 diacids are most abundant among
469 C_3-C_8 diacids determined during the photochemical oxidation of C_6-C_9 diacids in a laboratory
470 experiment (Yang et al., 2008a).
471 On the contrary, enhanced degradation of C_2 and C_3 and formation of C_4 diacid upon
472 prolonged irradiation, are not consistent with previous laboratory, observation and model
473 studies on photochemical production and degradation of diacids and related compounds in
474 aqueous phase (e.g., cloud processing) (Kawamura et al., 1996a; Kawamura and Sakaguchi,
475 1999; Warneck, 2003; Ervens et al., 2004b; Lim et al., 2005; Carlton et al., 2007;
476 Charbouillot et al., 2012). In fact, previous studies did not consider Fe-catalyzed photolysis
477 of C_2 diacid, which is significant at least in Fe-rich atmospheric waters. On the other hand,
478 the formation processes and potential precursor compounds of C_4 diacid have not been fully
479 explored yet. Moreover, previous laboratory experiments on aqueous solutions of specific
480 species did not consider the mixing state of organic and inorganic constituents in atmospheric

aerosols (Ervens et al., 2011), although simplified experiments sometimes provide useful information on mechanisms.

Generally, it has been considered that the anthropogenic contributions of α-dicarbonyls to organic aerosols are minor: 8% for Gly and 5% for MeGly (Fu et al., 2008). To the best of our knowledge, their production in atmospheric waters has not well been recognized yet. Our laboratory experiments indicate that the photochemical production of Gly and MeGly is significant in aqueous aerosols. The production of MeGly is more pronounced compared to Gly with prolonged photochemical processing of aqueous anthropogenic aerosols. Finally, our findings based on the batch laboratory experiment emphasize the importance of the photolysis of C_2 and C_3 diacids and photochemical production of C_4 diacid and α-dicarbonyls in aqueous aerosols to reconcile the current atmospheric model(s) such as cloud parcel model (Ervens et al., 2004a), and to better understand the secondary organic aerosol budget and its climatic impacts.

4 Summary and conclusions

In this study, we conducted batch UV irradiation experiments on anthropogenic (AA) and biogenic (BA) aerosol samples collected from Chennai, India in the presence of moisture for the reaction time of 0.5 h to 120 h. The irradiated samples were analyzed for molecular compositions of diacids, oxoacids and α-dicarbonyls. Concentrations of C_2 and C_3 and C_8-C_{12} diacids decreased with an increase in 12-24 h. In contrast, C_4 diacid (and C_5-C_7) showed a significant increase with reaction time up to 72 h in BA and 96 h in AA. Oxoacids and α-dicarbonyls showed a significant increase during an early stage of irradiation followed by a gradual decrease in the prolonged experiment, except for ωC_8 acid that showed a pattern similar to C_4 diacid and for methylglyoxal that remained relatively abundant from 24 h to the end of the experiment in AA. The mass ratios of C_2 diacid to its precursors: glyoxylic acid,

506 pyruvic acid, α-dicarbonyls (glyoxyal and methylglyoxal) and C_3, showed a considerable
507 increase with irradiation, while those of C_4 to C_5-C_7 diacids and ωC_8 acid and methylglyoxal
508 to glyoxal in AA showed a significant increase with irradiation. These results demonstrate
509 that degradation of C_2 and C_3 (and C_8-C_{12}) and formation of C_4 (and C_5-C_7) is enhanced with
510 photochemical processing of aqueous aerosols. This study further infers that iron-catalyzed
511 photolysis of C_2 and C_3 diacids and photochemical formation of C_4 diacid via ωC_8 acid
512 derived from cyclic olefins and/or unsaturated fatty acids play an important role in
513 controlling their abundances in the atmosphere with photochemical processing of aqueous
514 aerosols. This study also suggests that photochemical production of α-dicarbonyls, in
515 particular methylglyoxal, in anthropogenic aerosols is significant.
516
517 ***Acknowledgements.*** This study was in part supported by the Japan Society for the Promotion
518 of Science (JSPS) (Grant-in-aid Nos.19204055 and 24221001). C. M. Pavuluri appreciates
519 the financial support from JSPS Fellowship. The authors appreciate the helpful comments of
520 two anonymous reviewers.

References

Albrecht, B. A.: Aerosols, Cloud Microphysics, and Fractional Cloudiness, Science, 245, 1227-1230, 1989.

Arakaki, T. and Faust, B. C.: Sources, Sinks, and Mechanisms of Hydroxyl Radical (•Oh) Photoproduction and Consumption in Authentic Acidic Continental Cloud Waters from Whiteface Mountain, New York: The Role of the Fe(R) (R=Ii, III) Photochemical Cycle, J Geophys Res-Atmos, 103, 3487-3504, 1998.

Bandow, H., Washida, N. and Akimoto, H.: Ring-Cleavage Reactions of Aromatic-Hydrocarbons Studied by Ft-Ir Spectroscopy .1. Photooxidation of Toluene and Benzene in the Nox-Air System, B Chem Soc Jpn, 58, 2531-2540, 1985.

Carlton, A. G., Turpin, B. J., Lim, H. J., Altieri, K. E. and Seitzinger, S.: Link between Isoprene and Secondary Organic Aerosol (Soa): Pyruvic Acid Oxidation Yields Low Volatility Organic Acids in Clouds, Geophys Res Lett, 33, L06822, 2006.

Carlton, A. G., Turpin, B. J., Altieri, K. E., Seitzinger, S., Reff, A., Lim, H. J. and Ervens, B.: Atmospheric Oxalic Acid and Soa Production from Glyoxal: Results of Aqueous Photooxidation Experiments, Atmos Environ, 41, 7588-7602, 2007.

Charbouillot, T., Gorini, S., Voyard, G., Parazols, M., Brigante, M., Deguillaume, L., Delort, A. M. and Mailhot, G.: Mechanism of Carboxylic Acid Photooxidation in Atmospheric Aqueous Phase: Formation, Fate and Reactivity, Atmos Environ, 56, 1-8, 2012.

Chebbi, A. and Carlier, P.: Carboxylic Acids in the Troposphere, Occurrence, Sources, and Sinks: A Review, Atmos Environ, 30, 4233-4249, 1996.

Chitose, N., Ueta, S., Seino, S. and Yamamoto, T. A.: Radiolysis of Aqueous Phenol Solutions with Nanoparticles. 1. Phenol Degradation and Toc Removal in Solutions Containing Tio2 Induced by Uv, Gamma-Ray and Electron Beams, Chemosphere, 50, 1007-1013, 2003.

Ervens, B., Feingold, G., Clegg, S. L. and Kreidenweis, S. M.: A Modeling Study of Aqueous Production of Dicarboxylic Acids: 2. Implications for Cloud Microphysics, J Geophys Res-Atmos, 109, 2004a.

Ervens, B., Feingold, G., Frost, G. J. and Kreidenweis, S. M.: A Modeling Study of Aqueous Production of Dicarboxylic Acids: 1. Chemical Pathways and Speciated Organic Mass Production, J Geophys Res-Atmos, 109, D15205, doi: 10.1029/2003jd004387, 2004b.

553 Ervens, B., Turpin, B. J. and Weber, R. J.: Secondary Organic Aerosol Formation in Cloud
554 Droplets and Aqueous Particles (Aqsoa): A Review of Laboratory, Field and Model
555 Studies, Atmos Chem Phys, 11, 11069-11102, 2011.
556 Fu, P. Q., Kawamura, K., Pavuluri, C. M., Swaminathan, T. and Chen, J.: Molecular
557 Characterization of Urban Organic Aerosol in Tropical India: Contributions of Primary
558 Emissions and Secondary Photooxidation, Atmos Chem Phys, 10, 2663-2689, 2010.
559 Fu, T. M., Jacob, D. J., Wittrock, F., Burrows, J. P., Vrekoussis, M. and Henze, D. K.: Global
560 Budgets of Atmospheric Glyoxal and Methylglyoxal, and Implications for Formation of
561 Secondary Organic Aerosols, J Geophys Res-Atmos, 113, D15303, 2008.
562 Gao, S., Keywood, M., Ng, N. L., Surratt, J., Varutbangkul, V., Bahreini, R., Flagan, R. C.
563 and Seinfeld, J. H.: Low-Molecular-Weight and Oligomeric Components in Secondary
564 Organic Aerosol from the Ozonolysis of Cycloalkenes and A-Pinene, J Phys Chem A,
565 108, 10147-10164, 2004.
566 Garg, A., Bhattacharya, S., Shukla, P. R. and Dadhwal, W. K.: Regional and Sectoral
567 Assessment of Greenhouse Gas Emissions in India, Atmos Environ, 35, 2679-2695, 2001.
568 Giebl, H., Berner, A., Reischl, G., Puxbaum, H., Kasper-Giebl, A. and Hitzenberger, R.: Ccn
569 Activation of Oxalic and Malonic Acid Test Aerosols with the University of Vienna
570 Cloud Condensation Nuclei Counter, J Aerosol Sci, 33, 1623-1634, 2002.
571 Harvey, G. R., Boran, D. A., Chesal, L. A. and Tokar, J. M.: The Structure of Marine Fulvic
572 and Humic Acids, Mar Chem, 12, 119-132, 1983.
573 Hatakeyama, S., Ohno, M., Weng, J. H., Takagi, H. and Akimoto, H.: Mechanism for the
574 Formation of Gaseous and Particulate Products from Ozone-Cycloalkene Reactions in Air,
575 Environ Sci Technol, 21, 52-57, 1987.
576 Kalberer, M., Yu, J., Cocker, D. R., Flagan, R. C. and Seinfeld, J. H.: Aerosol Formation in
577 the Cyclohexene-Ozone System, Environ Sci Technol, 34, 4894-4901, 2000.
578 Kanakidou, M., Seinfeld, J. H., Pandis, S. N., Barnes, I., Dentener, F. J., Facchini, M. C., Van
579 Dingenen, R., Ervens, B., Nenes, A., Nielsen, C. J., Swietlicki, E., Putaud, J. P.,
580 Balkanski, Y., Fuzzi, S., Horth, J., Moortgat, G. K., Winterhalter, R., Myhre, C. E. L.,
581 Tsigaridis, K., Vignati, E., Stephanou, E. G. and Wilson, J.: Organic Aerosol and Global
582 Climate Modelling: A Review, Atmos. Chem. Phys., 5, 1053-1123, 2005.
583 Kawamura, K. and Gagosian, R. B.: Implications of Ω-Oxocarboxylic Acids in the Remote
584 Marine Atmosphere for Photooxidation of Unsaturated Fatty Acids, Nature, 325, 330-332,
585 1987.

586 Kawamura, K. and Kaplan, I. R.: Motor Exhaust Emissions as a Primary Source for
587 Dicarboxylic-Acids in Los-Angeles Ambient Air, Environ Sci Technol, 21, 105-110,
588 1987.
589 Kawamura, K.: Identification of C2-C10 Ω-Oxocarboxylic Acids, Pyruvic Acid, and C2-C3
590 A-Dicarbonyls in Wet Precipitation and Aerosol Samples by Capillary Gc and Gc/Ms,
591 Analytical Chemistry, 65, 3505-3511, 1993.
592 Kawamura, K. and Ikushima, K.: Seasonal Changes in the Distribution of Dicarboxylic Acids
593 in the Urban Atmosphere, Environ Sci Technol, 27, 2227-2235, 1993.
594 Kawamura, K., Kasukabe, H. and Barrie, L. A.: Source and Reaction Pathways of
595 Dicarboxylic Acids, Ketoacids and Dicarbonyls in Arctic Aerosols: One Year of
596 Observations, Atmos. Environ., 30, 1709-1722, 1996a.
597 Kawamura, K., Sempéré, R., Imai, Y., Fujii, Y. and Hayashi, M.: Water Soluble Dicarboxylic
598 Acids and Related Compounds in Antarctic Aerosols, J Geophys Res-Atmos, 101,
599 18721-18728, 1996b.
600 Kawamura, K. and Sakaguchi, F.: Molecular Distributions of Water Soluble Dicarboxylic
601 Acids in Marine Aerosols over the Pacific Ocean Including Tropics, J. Geophys. Res.,
602 [Atmos], 104, D3, 3501-3509, 1999.
603 Kawamura, K., Yokoyama, K., Fujii, Y. and Watanabe, O.: A Greenland Ice Core Record of
604 Low Molecular Weight Dicarboxylic Acids, Ketocarboxylic Acids, and
605 Alpha-Dicarbonyls: A Trend from Little Ice Age to the Present (1540 to 1989 Ad), J.
606 Geophys. Res., [Atmos], 106, 1331-1345, 2001.
607 Kawamura, K., Kasukabe, H. and Barrie, L. A.: Secondary Formation of Water-Soluble
608 Organic Acids and A-Dicarbonyls and Their Contributions to Total Carbon and
609 Water-Soluble Organic Carbon: Photochemical Aging of Organic Aerosols in the Arctic
610 Spring, J Geophys Res-Atmos, 115, D21306 DOI: 21310.21029/22010JD014299, 2010.
611 Kawamura, K., Ono, K., Tachibana, E., Charriére, B. and Sempéré, R.: Distributions of Low
612 Molecular Weight Dicarboxylic Acids, Ketoacids and A-Dicarbonyls in the Marine
613 Aerosols Collected over the Arctic Ocean During Late Summer, Biogeosciences, 9,
614 4725-4737, 2012.
615 Lelieveld, J., Crutzen, P. J., Ramanathan, V., Andreae, M. O., Brenninkmeijer, C. A. M.,
616 Campos, T., Cass, G. R., Dickerson, R. R., Fischer, H., de Gouw, J. A., Hansel, A.,
617 Jefferson, A., Kley, D., de Laat, A. T. J., Lal, S., Lawrence, M. G., Lobert, J. M.,
618 Mayol-Bracero, O. L., Mitra, A. P., Novakov, T., Oltmans, S. J., Prather, K. A., Reiner,
619 T., Rodhe, H., Scheeren, H. A., Sikka, D. and Williams, J.: The Indian Ocean Experiment:

620 Widespread Air Pollution from South and Southeast Asia, Science, 291, 1031-1036,
621 2001.
622 Lim, H. J., Carlton, A. G. and Turpin, B. J.: Isoprene Forms Secondary Organic Aerosol
623 through Cloud Processing: Model Simulations, Environ Sci Technol, 39, 4441-4446,
624 2005.
625 Lim, Y. B., Tan, Y., Perri, M. J., Seitzinger, S. P. and Turpin, B. J.: Aqueous Chemistry and
626 Its Role in Secondary Organic Aerosol (Soa) Formation, Atmos Chem Phys, 10,
627 10521-10539, 2010.
628 Mahowald, N., Jickells, T. D., Baker, A. R., Artaxo, P., Benitez-Nelson, C. R., Bergametti,
629 G., Bond, T. C., Chen, Y., Cohen, D. D., Herut, B., Kubilay, N., Losno, R., Luo, C.,
630 Maenhaut, W., McGee, K. A., Okin, G. S., Siefert, R. L. and Tsukuda, S.: Global
631 Distribution of Atmospheric Phosphorus Sources, Concentrations, and Deposition Rates,
632 and Anthropogenic Impacts, Global Biogeochem Cy, 22, 2008.
633 Matsunaga, S., Kawamura, K., Nakatsuka, T. and Ohkouchi, N.: Preliminary Study on
634 Laboratory Photochemical Formation of Low Molecular Weight Dicarboxylic Acids from
635 Unsaturated Fatty Acid (Oleic Acid), Res. Org. Geochem., 14, 19-25, 1999.
636 Narukawa, M., Kawamura, K., Takeuchi, N. and Nakajima, T.: Distribution of Dicarboxylic
637 Acids and Carbon Isotopic Compositions in Aerosols from 1997 Indonesian Forest Fires,
638 Geophys. Res. Lett., 26, 3101-3104, 1999.
639 Noziere, B., Ekstrom, S., Alsberg, T. and Holmstrom, S.: Radical-Initiated Formation of
640 Organosulfates and Surfactants in Atmospheric Aerosols, Geophys Res Lett, 37, 2010.
641 Pacyna, J. M. and Pacyna, E. G.: An Assessment of Global and Regional Emissions of Trace
642 Metals to the Atmosphere from Anthropogenic Sources Worldwide, Environmental
643 Reviews, 9, 269-298, 2001.
644 Padhy, P. K. and Varshney, C. K.: Emission of Volatile Organic Compounds (Voc) from
645 Tropical Plant Species in India, Chemosphere, 59, 1643-1653, 2005.
646 Pavuluri, C. M., Kawamura, K. and Swaminathan, T.: Water-Soluble Organic Carbon,
647 Dicarboxylic Acids, Ketoacids, and Alpha-Dicarbonyls in the Tropical Indian Aerosols, J
648 Geophys Res-Atmos, 115, doi:10.1029/2009jd012661, 2010.
649 Pavuluri, C. M., Kawamura, K., Aggarwal, S. G. and Swaminathan, T.: Characteristics,
650 Seasonality and Sources of Carbonaceous and Ionic Components in the Tropical Aerosols
651 from Indian Region, Atmos Chem Phys, 11, 8215-8230, 2011.
652 Pavuluri, C. M. and Kawamura, K.: Evidence for 13-Carbon Enrichment in Oxalic Acid Via
653 Iron Catalyzed Photolysis in Aqueous Phase, Geophys Res Lett, 39, 2012.

654 Reddy, M. S. and Venkataraman, C.: Inventory of Aerosol and Sulphur Dioxide Emissions
655 from India: I - Fossil Fuel Combustion, Atmos Environ, 36, 677-697, 2002a.
656 Reddy, M. S. and Venkataraman, C.: Inventory of Aerosol and Sulphur Dioxide Emissions
657 from India. Part Ii - Biomass Combustion, Atmos Environ, 36, 699-712, 2002b.
658 Saxena, P. and Hildemann, L. M.: Water-Soluble Organics in Atmospheric Particles: A
659 Critical Review of the Literature and Application of Thermodynamics to Identify
660 Candidate Compounds, J. Atmos. Chem., 24, 57-109, 1996.
661 Shirayama, H., Tohezo, Y. and Taguchi, S.: Photodegradation of Chlorinated Hydrocarbons
662 in the Presence and Absence of Dissolved Oxygen in Water, Water Res, 35, 1941-1950,
663 2001.
664 Solmon, F., Chuang, P. Y., Meskhidze, N. and Chen, Y.: Acidic Processing of Mineral Dust
665 Iron by Anthropogenic Compounds over the North Pacific Ocean, J Geophys Res-Atmos,
666 114, 2009.
667 Sorooshian, A., Wang, Z., Coggon, M. M., Jonsson, H. H. and Ervens, B.: Observations of
668 Sharp Oxalate Reductions in Stratocumulus Clouds at Variable Altitudes: Organic Acid
669 and Metal Measurements During the 2011 E-Peace Campaign, Environ Sci Technol, 47,
670 7747-7756, 2013.
671 Srinivas, B., Sarin, M. M. and Kumar, A.: Impact of Anthropogenic Sources on Aerosol Iron
672 Solubility over the Bay of Bengal and the Arabian Sea, Biogeochemistry, 110, 257-268,
673 2012.
674 Stookey, L. C.: Ferrozine - a New Spectrophotometric Reagent for Iron, Anal Chem, 42,
675 779-781, 1970.
676 Tan, Y., Perri, M. J., Seitzinger, S. P. and Turpin, B. J.: Effects of Precursor Concentration
677 and Acidic Sulfate in Aqueous Glyoxal-Oh Radical Oxidation and Implications for
678 Secondary Organic Aerosol, Environ Sci Technol, 43, 8105-8112, 2009.
679 Tan, Y., Lim, Y. B., Altieri, K. E., Seitzinger, S. P. and Turpin, B. J.: Mechanisms Leading to
680 Oligomers and Soa through Aqueous Photooxidation: Insights from Oh Radical Oxidation
681 of Acetic Acid and Methylglyoxal, Atmos Chem Phys, 12, 801-813, 2012.
682 Theodosi, C., Markaki, Z. and Mihalopoulos, N.: Iron Speciation, Solubility and Temporal
683 Variability in Wet and Dry Deposition in the Eastern Mediterranean, Mar Chem, 120,
684 100-107, 2010a.
685 Theodosi, C., Markaki, Z., Tselepides, A. and Mihalopoulos, N.: The Significance of
686 Atmospheric Inputs of Soluble and Particulate Major and Trace Metals to the Eastern
687 Mediterranean Seawater, Mar Chem, 120, 154-163, 2010b.

688 Tilgner, A. and Herrmann, H.: Radical-Driven Carbonyl-to-Acid Conversion and Acid
689 Degradation in Tropospheric Aqueous Systems Studied by Capram, Atmos Environ, 44,
690 5415-5422, 2010.
691 Twomey, S.: Influence of Pollution on Shortwave Albedo of Clouds, J Atmos Sci, 34,
692 1149-1152, 1977.
693 Wang, G., Xie, M., Hu, S., Gao, S., Tachibana, E. and Kawamura, K.: Dicarboxylic Acids,
694 Metals and Isotopic Compositions of C and N in Atmospheric Aerosols from Inland
695 China: Implications for Dust and Coal Burning Emission and Secondary Aerosol
696 Formation, Atmos Chem Phys, 10, 6087-6096, 2010a.
697 Wang, Z. H., Chen, X., Ji, H. W., Ma, W. H., Chen, C. C. and Zhao, J. C.: Photochemical
698 Cycling of Iron Mediated by Dicarboxylates: Special Effect of Malonate, Environ Sci
699 Technol, 44, 263-268, 2010b.
700 Warneck, P.: In-Cloud Chemistry Opens Pathway to the Formation of Oxalic Acid in the
701 Marine Atmosphere, Atmos Environ, 37, 2423-2427, 2003.
702 Weeks, J. L., Meaburn, G. M. and Gordon, S.: Absorption Coefficients of Liquid Water and
703 Aqueous Solutions in the Far Ultraviolet, Radiation research, 19, 559-567, 1963.
704 Wheeler, J.: Some Effects of Solar Levels of Ultraviolet-Radiation on Lipids in Artificial
705 Sea-Water, J Geophys Res, 77, 5302-5306, 1972.
706 Yang, L. M., Ray, M. B. and Yu, L. E.: Photooxidation of Dicarboxylic Acids- Part Ii:
707 Kinetics, Intermediates and Field Observations, Atmos Environ, 42, 868-880, 2008a.
708 Yang, L. M., Ray, M. B. and Yu, L. E.: Photooxidation of Dicarboxylic Acids- Part 1: Effects
709 of Inorganic Ions on Degradation of Azelaic Acid, Atmos Environ, 42, 856-867, 2008b.
710 Zuo, Y. G. and Hoigne, J.: Photochemical Decomposition of Oxalic, Glyoxalic and Pyruvic
711 Acid Catalyzed by Iron in Atmospheric Waters, Atmos Environ, 28, 1231-1239, 1994.
712
713

Table 1. Concentrations of carbonaceous components, organic molecular tracer compounds, diacids and related compounds, trace elements, metals and water-soluble iron species in non-irradiated IND104 (anthropogenic aerosols: AA) and IND178 (biogenic aerosols: BA) aerosol samples collected from Chennai, India.

	Concentrations (ng m^{-3})	
	IND104 (AA)	IND178 (BA)
Organic carbon[a]	6400	9820
Elemental carbon[a]	4810	1810
Levoglucosan[b]	79.1	158
Hopanes (C_{27}-C_{35}) [b]	11.8	3.9
Fatty acids (C_8-C_{34}) [b]	167	297
Fatty alcohols (C_{14}-C_{34}) [b]	93.3	178
Total diacids	1030	640
Total oxoaxids	110	62.2
Total α-dicarbonyls	10.9	11.6
Al	15100	914
Ca	1640	0.00
Cd	10.7	1.73
Co	1.07	0.00
Cr	5.33	0.00
Cu	796	13.9
Fe	2070	553
K	1220	893
Mg	679	90.2
Mn	129	19.1
Na	1890	408
Ni	58.7	106
P	62.9	0.00
Pb	133	39.9
S	4640	5820
Sb	13.9	29.5
V	9.60	0.00
Zn	2030	137
Fe_{WS}[c]	57.0	78.3
Fe^{2+}	20.5	30.0
Fe^{3+}	36.6	48.4

[a]: Data is obtained from Pavuluri et al. (2011), [b]: Data is obtained from Fu et al. (2010), [c]: Fe_{WS} is water-soluble Fe.

Figure Captions

Fig. 1. A map of South Asia with sampling site, Chennai (13.04°N; 80.17°E), India together with plots of 10-day air mass trajectories arriving at 500 m a.g.l. over Chennai, India.

Fig. 2. Schematic of experimental setup for irradiation of atmospheric aerosol filter sample.

Fig. 3. Changes in concentrations of individual dicarboxylic acids and total diacids as a function of UV irradiation time in anthropogenic (AA) and biogenic aerosols (BA).

Fig. 4. Changes in concentrations of individual oxoacids and α-dicarbonyls and total oxoacids and α-dicarbonyls as a function of UV irradiation time in AA and BA.

Fig. 5. Changes in relative abundances of straight chain diacids (C_2-C_{10}) to total diacids as a function of UV irradiation time in AA and BA.

Fig. 6. Changes in mass ratios of selected diacids, oxoacids and α-dicarbonyls as a function of UV irradiation time in AA and BA.

Fig. 7. Possible photochemical formation and/or degradation pathways of diacids, oxoacids and α-dicarbonyls in aqueous aerosols.

734 **Fig. 1.**

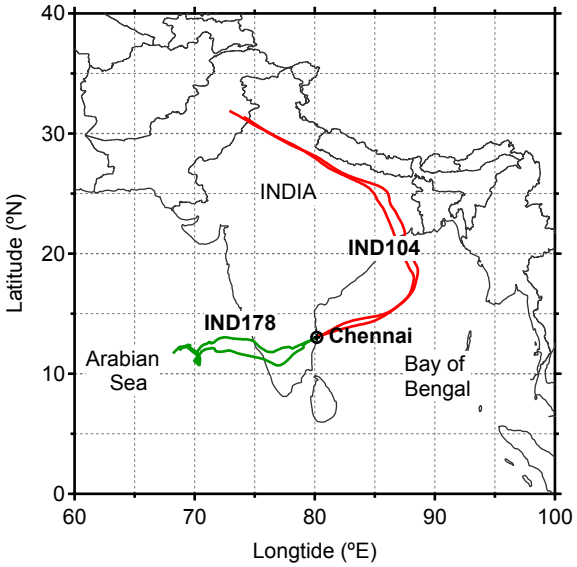
40
30
20
10
0
60
70
80
90
100
Latitude (°N)
Longtide (°E)
INDIA
IND104
IND178
Chennai
Arabian
Sea
Bay of
Bengal

735

736 **Fig. 2.**

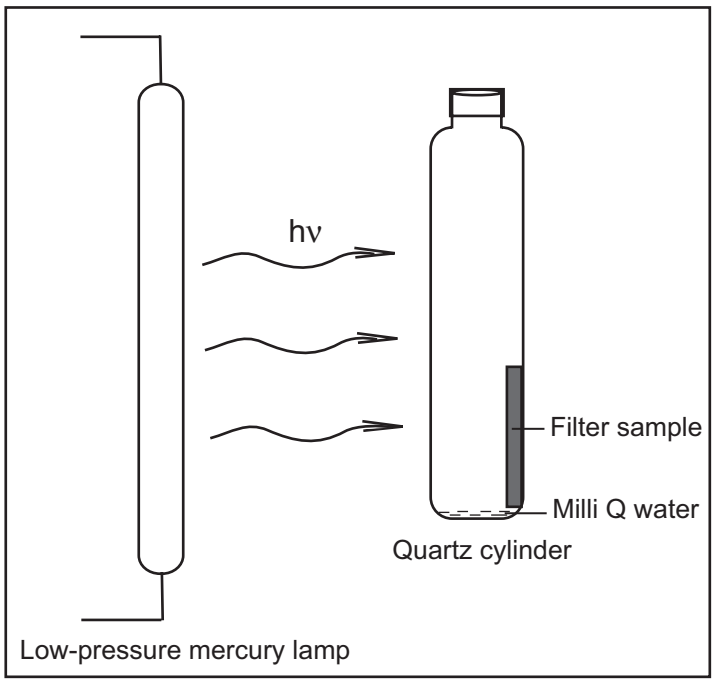
hν
Filter sample
Milli Q water
Quartz cylinder
Low-pressure mercury lamp

737

738 **Fig. 3.**

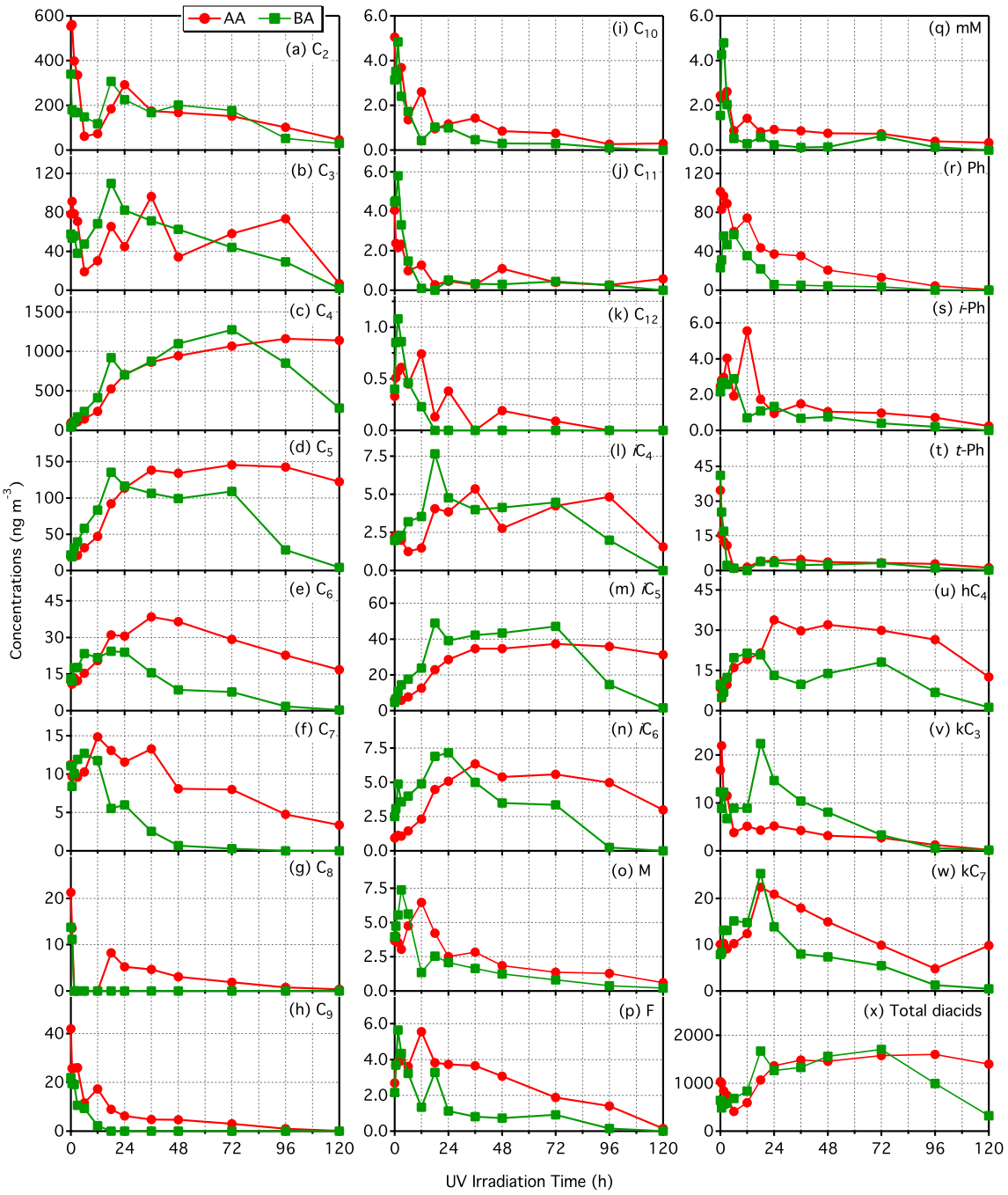
AA
BA
(a) C2
(b) C3
(c) C4
(d) C5
(e) C6
(f) C7
(g) C8
(h) C9
(i) C10
(j) C11
(k) C12
(l) iC4
(m) iC5
(n) iC6
(o) M
(p) F
(q) mM
(r) Ph
(s) i-Ph
(t) t-Ph
(u) hC4
(v) kC3
(w) kC7
(x) Total diacids
Concentrations (ng m-3)
UV Irradiation Time (h)

739

740 **Fig. 4.**

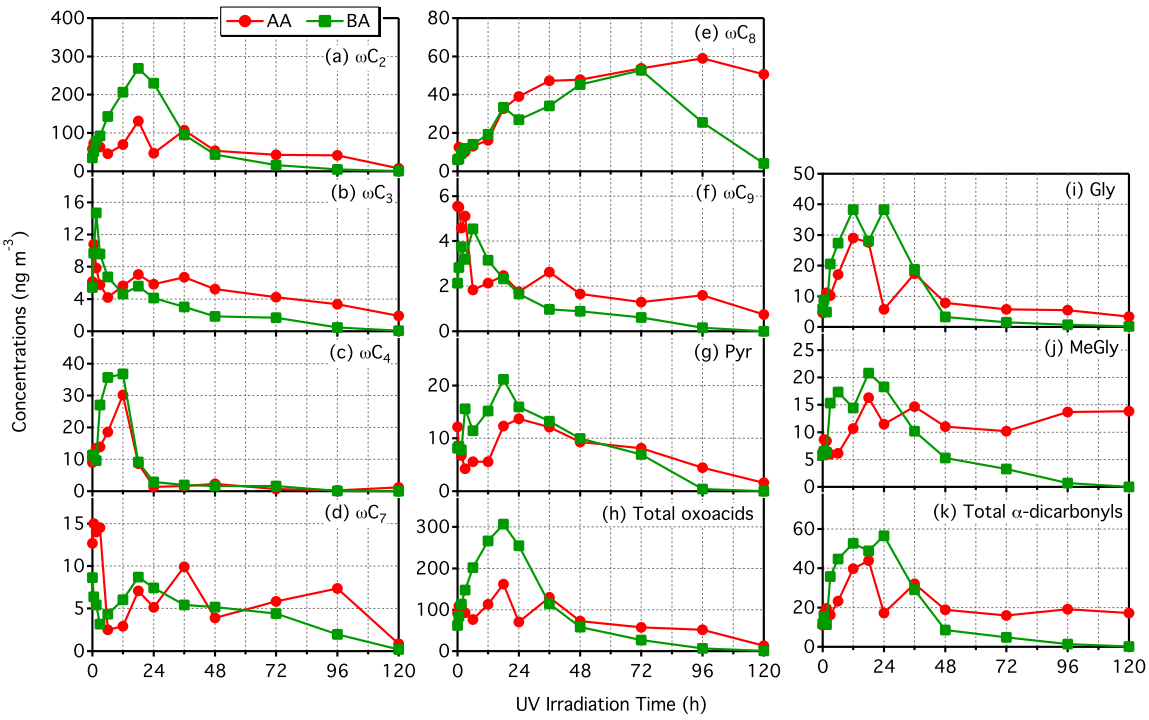
AA
BA
(a) ωC2
(b) ωC3
(c) ωC4
(d) ωC7
(e) ωC8
(f) ωC9
(g) Pyr
(h) Total oxoacids
(i) Gly
(j) MeGly
(k) Total α-dicarbonyls
Concentrations (ng m-3)
UV Irradiation Time (h)

741

742 **Fig. 5.**

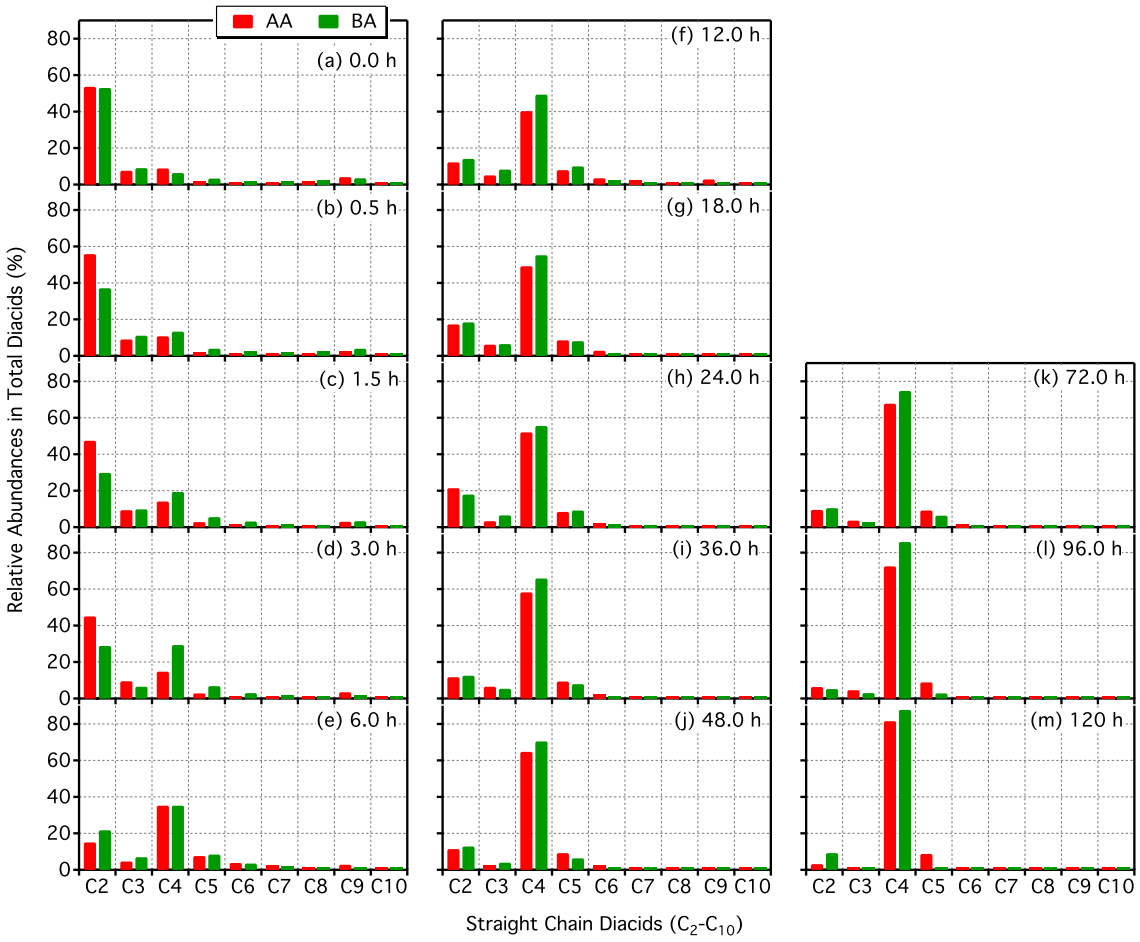
AA
BA
(a) 0.0 h
(b) 0.5 h
(c) 1.5 h
(d) 3.0 h
(e) 6.0 h
(f) 12.0 h
(g) 18.0 h
(h) 24.0 h
(i) 36.0 h
(j) 48.0 h
(k) 72.0 h
(l) 96.0 h
(m) 120 h
Relative Abundances in Total Diacids (%)
0
20
40
60
80
C2 C3 C4 C5 C6 C7 C8 C9 C10
Straight Chain Diacids (C2-C10)

743

744 **Fig. 6.**

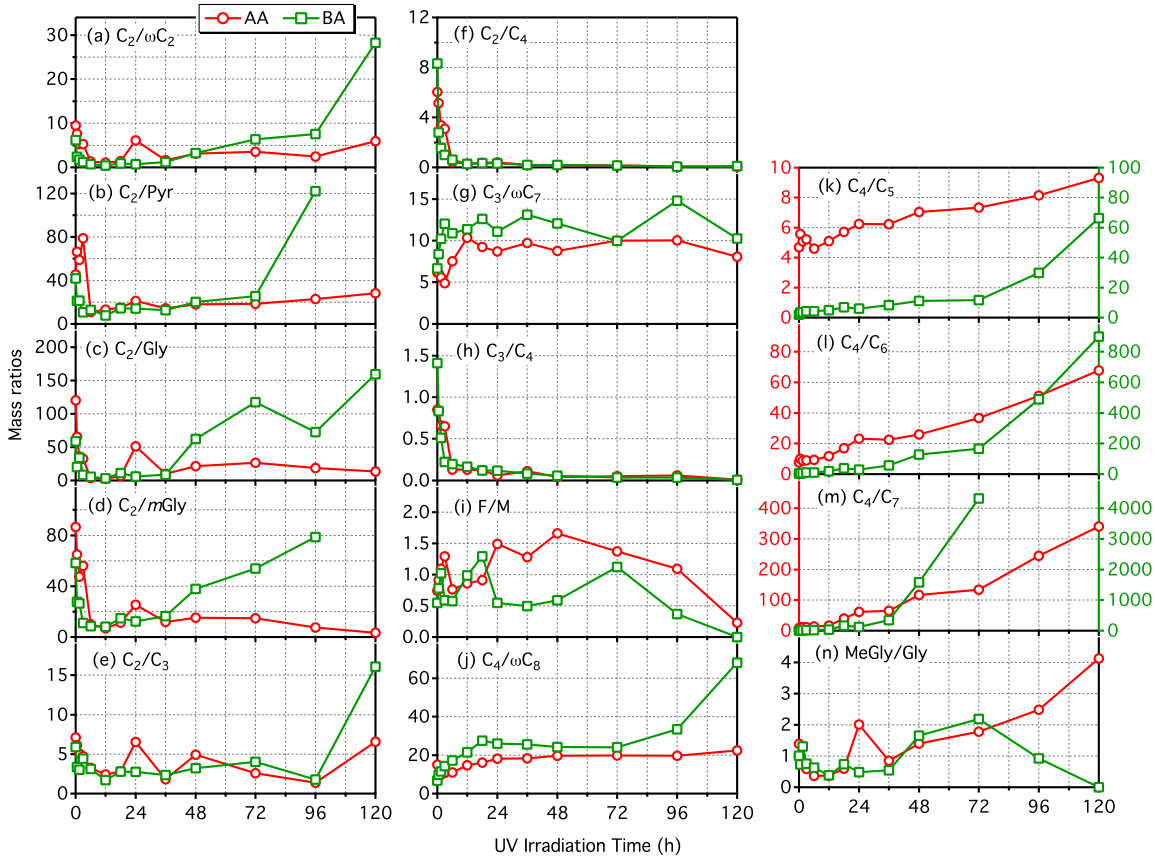
AA
BA
(a) C2/ωC2
(b) C2/Pyr
(c) C2/Gly
(d) C2/mGly
(e) C2/C3
(f) C2/C4
(g) C3/ωC7
(h) C3/C4
(i) F/M
(j) C4/ωC8
(k) C4/C5
(l) C4/C6
(m) C4/C7
(n) MeGly/Gly
Mass ratios
UV Irradiation Time (h)

745

746 **Fig. 7.**

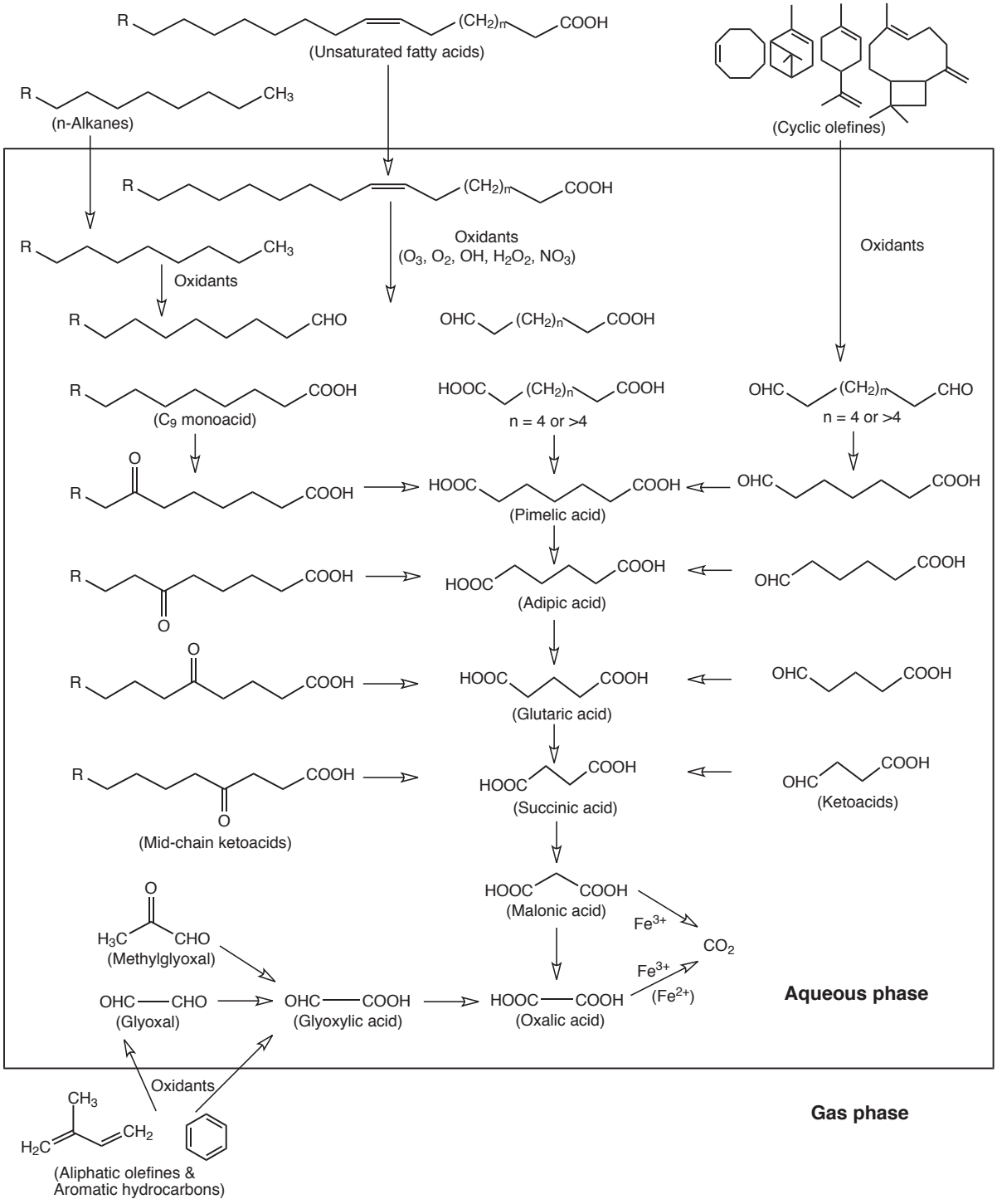
(Unsaturated fatty acids)
(n-Alkanes)
(Cyclic olefines)
Oxidants
(O3, O2, OH, H2O2, NO3)
Oxidants
Oxidants
(C9 monoacid)
n = 4 or >4
n = 4 or >4
(Pimelic acid)
(Adipic acid)
(Glutaric acid)
(Succinic acid)
(Ketoacids)
(Mid-chain ketoacids)
(Malonic acid)
(Methylglyoxal)
(Glyoxal)
(Glyoxylic acid)
(Oxalic acid)
Fe3+
Fe3+
(Fe2+)
CO2
Aqueous phase
Oxidants
Gas phase
(Aliphatic olefines &
Aromatic hydrocarbons)

747